Available online at www.sciencedirect.com
SCIENCE DIRECT®
ELSEVIER
Earth and Planetary Science Letters 218 (2004) 421–434
EPSL
www.elsevier.com/locate/epsl

Sharp decrease in long-term chemical weathering rates along an altitudinal transect☆

Clifford S. Riebe [a,*], James W. Kirchner [a], Robert C. Finkel [b,c]

[a] Department of Earth and Planetary Science, University of California, Berkeley, CA 94720-4767, USA
[b] Center for Accelerator Mass Spectrometry, Lawrence Livermore National Laboratory, Livermore, CA 94551, USA
[c] Department of Earth Science, University of California, Riverside, CA 92521, USA

Received 23 May 2003; received in revised form 16 October 2003; accepted 11 November 2003

Abstract

We used cosmogenic nuclide and geochemical mass balance methods to measure long-term rates of chemical weathering and physical erosion across a steep climatic gradient in the Santa Rosa Mountains, Nevada. Our study sites are distributed along a 2 km ridgeline transect that spans 2090 to 2750 m in altitude, and encompasses marked contrasts in both vegetative cover and snow depth, but is underlain by a single, roughly uniform, granodiorite bedrock. Cosmogenic nuclides in colluvial soils reveal that denudation rates vary by less than a factor of 1.4 (104–144 t/km^2/yr) along this transect. Bulk elemental analyses indicate that, relative to the parent rock, soils are less intensively weathered with increasing altitude, and show little evidence of weathering-related mass losses near the top of the ridge. Chemical weathering rates decrease rapidly with increasing altitude, both in absolute terms (from 24 to 0 t/km^2/yr) and as a fraction of total denudation rates (from 20 to 0%). Thus these results indicate an increasing dominance of physical erosion with altitude. The observed decrease in chemical weathering rates is greater than one would predict from the decrease in mean annual temperature using simple weathering kinetics, suggesting that weathering rates along our transect may also be affected by the progressive decline in vegetative cover and increase in snow depth with increasing altitude. These results, considered together with weathering rate measurements for a wide range of climates in the Sierra Nevada, USA, suggest that chemical weathering rates may be particularly sensitive to differences in climate at higher-altitude sites. Consistent with this hypothesis, chemical weathering rates fall virtually to zero at the highest sites on our transect, suggesting that sparsely vegetated, high-altitude crystalline terrain may often be characterized by extremely slow silicate weathering rates.

Keywords: chemical weathering rates; weathering-climate feedbacks; physical erosion rates; cosmogenic nuclides

1. Introduction

Chemical weathering supplies nutrients and solutes to soils, streams and the oceans and is thus an important component in many biogeochemical cycles. For example, silicate weathering is the dominant long-term sink for atmospheric CO_2 and thus the dominant regulator of the green-

* Corresponding author. Tel.: +1-510-643-2171; Fax: +1-510-643-9980.
E-mail addresses: riebe@seismo.berkeley.edu (C.S. Riebe), kirchner@seismo.berkeley.edu (J.W. Kirchner), finkell@llnl.gov (R.C. Finkel).

☆ Supplementary data associated with this article can be found at doi:10.1016/S0012-821X(03)00673-3

0012-821X/03/$ – see front matter
doi:10.1016/S0012-821X(03)00673-3

house effect over geologic timescales. Hence, quantifying how chemical weathering rates depend on both climatic and non-climatic factors is essential for understanding Earth's long-term climatic evolution (e.g., [1,2]).

Field studies indicate that chemical weathering rates are affected by climatic factors such as runoff [3,4], altitude [5], vegetation [6–8], precipitation [9,10], and temperature [10]. Field evidence also indicates that chemical weathering rates are often tightly coupled with physical erosion rates (e.g., [11–16]), which regulate the supply of weatherable minerals by setting the rate that rock is broken down and incorporated into soils. If chemical weathering rates depend strongly on rates of physical erosion, site-to-site variations in erosion rates can obscure the dependence of chemical weathering on climate [13,16]. However, in previous studies of climatic effects on weathering, the potentially confounding effects of variations in erosion rates have been largely ignored, because reliable measurements of rates of chemical weathering and physical erosion have rarely been located together.

Measurements of long-term physical erosion rates have recently become much more widely available through cosmogenic nuclide techniques (e.g., [17–22]). Moreover, it has now been shown that long-term chemical weathering rates can also be readily measured in eroding landscapes using cosmogenic nuclide measurements of denudation rates, in combination with a geochemical mass balance in which dissolution losses are inferred from the rock-to-soil enrichment of insoluble elements [13,16,23]. Hence, using these cosmogenic nuclide and geochemical mass balance methods together, it should now be possible to determine, with unprecedented resolution, the relative importance of climatic and non-climatic factors in regulating long-term chemical weathering rates [16].

We used this new, cosmogenic/mass balance approach to measure rates of chemical weathering and physical erosion at six sites along a 2 km long ridge in the Santa Rosa Mountains. This steep ridge provides an ideal setting for measuring climatic effects on chemical weathering, because its high relief creates large differences in climate over a short distance, thus minimizing lithologic differences among our sites. By remaining within a single lithology, and explicitly measuring physical erosion rates (using cosmogenic nuclides), we can at once minimize and effectively account for any site-to-site differences in rates that fresh minerals are supplied to soils. Our ridgeline transect spans 2090 to 2750 m in altitude (corresponding to 3.6 to −0.4°C in mean annual air temperature), and encompasses marked contrasts in both vegetative cover and snow depth. Our measurements indicate that denudation rates (and thus rates of mineral supply from conversion of rock to soil) do not vary systematically along the altitude transect, but chemical weathering rates decrease rapidly with increasing altitude, declining to almost zero near the top of the ridge. These results suggest that variations in climate, and corresponding variations in vegetation, can have pronounced effects on chemical weathering rates at high altitudes.

2. Field site

The Santa Rosa Mountains fault block of the northern Basin and Range, Nevada rises between the Quinn River basin and Paradise Valley, with peak elevations in the central granodioritic portion reaching as high as 2966 m and standing roughly 1400 m above the valley floors. Spur ridges of the Santa Rosa Mountains provide ideal locations for studying climatic effects on chemical weathering rates, because their high relief and steep slopes impose sharp climatic contrasts over short distances. Many of these ridges thus encompass a wide range of climates, while remaining within a single lithology, and thus minimize potentially confounding variations in bedrock weathering susceptibility. Here we report measurements from six locations spanning 660 m in relief along a granodioritic spur ridge separating the North and South Forks of Hanson Creek (Fig. 1).

All of our sampling sites are on or near the crest of the spur ridge, with minimal contributing areas (<1 ha). Soils are derived from underlying bedrock or transported from within tens of meters upslope, lack visible horizonation, and are uni-

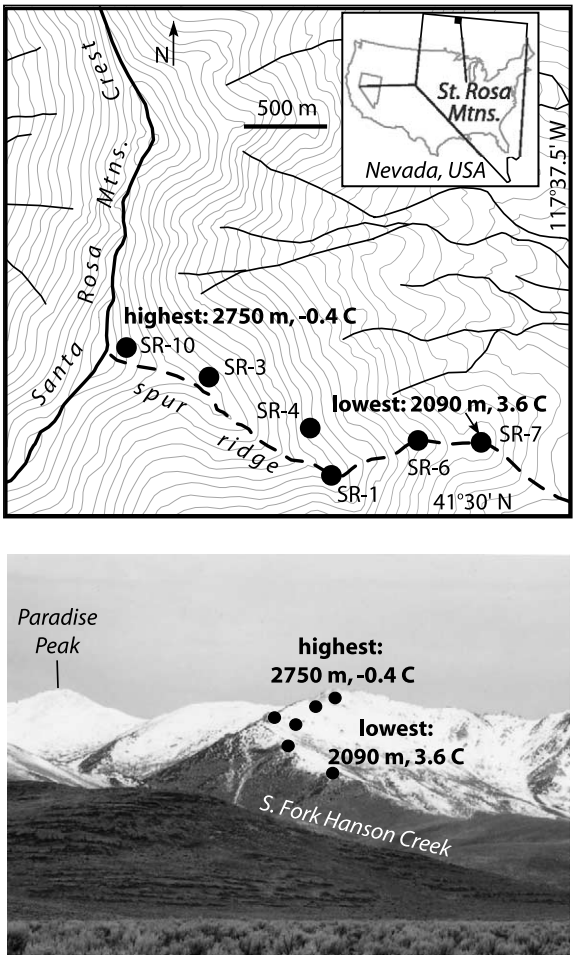

Fig. 1. Map (top, with contour interval = 30 m) and picture (bottom, taken from Paradise Valley, NV) showing sampling sites (circles) along the Hanson Creek spur ridge of the Santa Rosa Mountains. Note that all sites are at or near the top of the ridgecrest. Hence, even the study sites that are not located directly on the ridgeline (SR-10, 3 and 4) encompass very small catchments, with contributing areas <1 ha.

formly thin (<60 cm), mantling coherent saprolite that retains much of the bedrock's structure and mechanical strength. Soils from the higher sites along the transect generally exhibit a decrease in the amount of visible organic matter and increasingly abundant proportions of fresh-looking mineral grains. During rainstorms at a similar, sparsely vegetated, granitic site, also in the Basin and Range nearby, we have observed abundant detachment and transport of surface material due to the impact of rain, suggesting that rainsplash may also be an important sediment transport process at the Santa Rosa Mountains sites. Abundant burrows on slopes attest to active excavation and downslope transport of the grussy soils by insects and animals, which possibly also help incorporate saprolite into soil, although no unequivocal evidence of this was observed. During a site visit in late winter 2003, we observed a noticeable decrease in the density of surface material underfoot, compared to what we observed the summer before, presumably due to freeze–thaw-related heave and transport of soil. Shallow landsliding is likely to be locally important in steep, convergent areas, but less important on the relatively gentle, convex ridges and small catchments such as those considered here.

Using a lapse rate of -6°C/km, along with 55 years of temperature data from nearby Winnemucca, Nevada, we infer that mean annual temperatures at the base and top of the transect are 3.6 and -0.4°C, respectively. In situ soil temperature probes, logged at half-hour intervals and averaged over a recent 7 month period, indicate that temperatures at the soil/saprolite boundary decline by roughly 4.3°C from the bottom to the top of the transect, roughly consistent with the assumed air temperature lapse rate. Average annual precipitation, based on isoheyetal maps interpolated from nearby weather station data [24], ranges from approximately 65 cm/yr at the base to 85 cm/yr at the top of the Santa Rosa Mountains transect. Orographic effects lead to significant variability in the extent and depth of snow cover in Basin and Range mountains, and although this is difficult to quantify specifically for the Santa Rosa Mountains in the absence of long-term monitoring data, we observed that snow depths ranged from 0–10 cm near the base to >2 m in hollows near the top of the transect during early March, 2003 (see photograph in Fig. 1). Moreover, our soil temperature data indicate that soils thaw progressively later with increasing altitude (by as much as 3 months later at the top of the transect than at the bottom), suggesting that freezing temperatures and snow cover persist longer on average at higher altitudes. The observed differences in snow cover and timing of

spring thaw could be due to differences in the absolute amount of precipitation, differences in the proportion of precipitation that falls as snow, differences in rates of sublimation and snowmelt, or a combination of all three.

Vegetation varies both in type and density, from sparse decimeter-high sagebrush (*Artemisia*) near the top, to a mixture of dense, 1 m high *Artemisia* and *Ceanothus* and 2–3 m tall aspen (*Populus tremuloides*) near the base of the transect. Evidence of cattle grazing on slopes and ridges implies that vegetation distribution and density may have been altered somewhat by recent land use, and therefore may not exactly reflect conditions that have applied over the long (i.e., 10^3 year) timescales of our cosmogenic nuclide measurements. Although we cannot precisely quantify the likely extent of land-use-induced vegetation changes along the transect, we expect that the lower sites have probably been affected most, because they are more accessible to cattle for a greater part of the year (due to the differences in snow cover). Hence, if anything, we expect that the progressive, altitudinal decline in vegetation density over the long term may have been even sharper than what we observe today. In any case, the observed, inferred and implied differences in vegetation, temperature, precipitation, snow cover and timing of thaw together suggest that climatic conditions for weathering and erosion vary significantly along our transect.

3. Measuring long-term chemical weathering rates in eroding landscapes

3.1. The relationship between chemical weathering rates and immobile element enrichment in eroding landscapes

Long-term chemical weathering rates have typically been estimated using a mass balance approach [25,26], in which chemical weathering outputs are inferred from the changes wrought in parent material as it is converted to weathered soil. Geochemical mass balance methods infer chemical weathering losses by measuring the enrichment of immobile elements in the weathered material. Elements that are immobile during chemical weathering become enriched as other elements are removed by dissolution; the greater the mass lost through dissolution, the greater the relative enrichment of the immobile elements that are left behind. Soil mass balance approaches based on immobile element enrichment have typically only been applied to non-eroding soils of known age. However, recent work has shown that they can also be applied in mountainous settings where soils are undergoing significant physical erosion [13,16,23].

For a soil undergoing steady-state formation, erosion, and weathering (such that the mass of weathered material in storage as soil on the landscape is approximately constant through time) conservation of mass implies that the soil production rate will be equal to the total denudation rate. For such soils, it can be shown [13,16] that:

$$W = D\left(1-\frac{[\mathrm{Zr}]_{\mathrm{rock}}}{[\mathrm{Zr}]_{\mathrm{soil}}}\right) \quad (1)$$

where W is the chemical weathering flux from the soil as a whole and D is the total denudation flux (i.e., the sum of the physical erosion and chemical weathering fluxes), both in units of mass per area per time, and $[\mathrm{Zr}]_{\mathrm{rock}}$ and $[\mathrm{Zr}]_{\mathrm{soil}}$ are the concentrations of an immobile element (in this case zirconium) in rock and soil. In Eq. 1, the denudation rate D is expressed as a mass flux for dimensional consistency with the weathering flux. Denudation rates are often reported in the literature in units of length per time, reflecting rates of landscape lowering. These can be straightforwardly scaled by parent material density to yield the denudation mass flux used in our analysis.

Eq. 1 can be rearranged to yield:

$$\frac{W}{D} = \left(1-\frac{[\mathrm{Zr}]_{\mathrm{rock}}}{[\mathrm{Zr}]_{\mathrm{soil}}}\right) = \mathrm{CDF} \quad (2)$$

where CDF, the 'chemical depletion fraction', is the fraction of total denudation that is accounted for by chemical weathering [13,16].

Conservation of mass equations can also be written for individual elements in the rock and soil, yielding equations for weathering rates of individual elements:

$$W_X = D\left([X]_{rock} - [X]_{soil}\frac{[Zr]_{rock}}{[Zr]_{soil}}\right) \quad (3)$$

where $[X]_{rock}$ and $[X]_{soil}$ are the concentrations of an element X in rock and soil, and W_X is its chemical weathering rate [13,16,23].

The weathering rate W_X can be expressed in non-dimensional form as:

$$\frac{W_X}{D[X]_{rock}} = \left(1 - \frac{[X]_{soil}}{[X]_{rock}}\frac{[Zr]_{rock}}{[Zr]_{soil}}\right) = CDF_X \quad (4)$$

where CDF_X, the CDF of element X, expresses the element's chemical weathering rate as a fraction of its total denudation rate [16]. Note that CDF_X also corresponds to the negative of the mass transfer coefficient for weathering of element X in the approach of Brimhall et al. ([27,28], see also [14,26,29]).

The Appendix[1] includes additional details on the derivation of Eqs. 1–4.

3.2. Quantifying denudation rates with cosmogenic nuclides

The geochemical mass balance of Eqs. 1–4 yields chemical weathering rates of soils and their component elements from measurements of immobile element enrichment, concentrations of constituent elements in rock and soil, and total denudation rates. Denudational mass flux rates (i.e., D in Eqs. 1–4) can be measured, over timescales comparable to those of soil formation, using cosmogenic nuclide methods. Because these methods have come into widespread use only in the past few years, geochemical mass balance methods have only recently become applicable to eroding landscapes [13,16,23].

^{10}Be is produced in quartz grains near the Earth's surface by cosmic ray neutrons and muons (e.g., [17]). Because quartz grains at depth are shielded from cosmic radiation, cosmogenic ^{10}Be concentrations in quartz grains reflect their near-surface residence times, and can be used to infer long-term average rates of outcrop erosion [17], landscape denudation [18–20], and soil production [21,30]. Denudation rates from cosmogenic nuclides are averaged over roughly the timescale required to erode 160 g/cm^2 of material, or about 60 cm for rock with density 2.6 g/cm^3. For a soil of density 1.3 g/cm^3, 160 g/cm^2 corresponds to an equivalent soil thickness of about 120 cm, which is more than two times greater than typical soil depths in the Santa Rosa Mountains. Hence, denudation rates from cosmogenic nuclides will typically be averaged over at least two soil residence times and are therefore well suited for quantifying soil formation rates. Details of how cosmogenic nuclide measurements can be used to infer denudation rates (D) for use in Eqs. 1–4 have been presented in previous work (e.g., [16,31]) and are included in the electronic appendix.

3.3. Sampling and analysis

We collected widely distributed samples of soil and parent material (each roughly 0.5 kg) from 0.5–1.0 ha areas at six sites along our Santa Rosa Mountains climate transect (Fig. 1). Our aim was to capture any local variability in chemical weathering at each of these sites, and to avoid sampling from single, potentially anomalous points on the landscape, while still sampling a narrow elevation range at each site, so that each site would represent a distinct set of climatic conditions. We sampled soils both from surfaces and also from depth, in order to account for potential biases due to vertical sorting by physical processes. Outcrops were sampled to represent the parent material from which the local soils were formed. This should be a valid approach for sampling parent material, given that mineral alteration in outcrops at the Santa Rosa Mountains transect is generally limited to slight discoloration and oxidation staining (and is therefore unlikely to entail significant chemical weathering mass losses). In all we obtained 49 samples of soil, six samples of saprolite (from the bases of several soil pits), and 28 samples of parent rock.

We dried the samples at ~110°C for 12 h, then used sample splitters to subsample ~30 g each for analysis by X-ray fluorescence (XRF). Each subsample was powdered in a tungsten carbide grinding mill for ~5 min (resulting grain size:

[1] See online version of this article.

Table 1
Average element concentrations (Rb, Sr, Y, and Zr, in ppm, all others in percent)[a]

Element	SR-7 (2086 m)		SR-6 (2180 m)			SR-4 (2350 m)		SR-1 (2377 m)			SR-3 (2580 m)		SR-10 (2749 m)	
	soil	rock	soil	saprolite	rock	soil	rock	soil	saprolite	rock	soil	rock	soil	rock
[Na]	1.53 ± 0.03	1.74 ± 0.01	1.44 ± 0.01	1.71 ± 0.07	1.78 ± 0.01	1.59 ± 0.01	1.77 ± 0.03	1.56 ± 0.01	1.73 ± 0.06	1.76 ± 0.01	1.46 ± 0.03	1.68 ± 0.02	1.38 ± 0.01	1.67 ± 0.02
[Mg]	0.81 ± 0.03	0.97 ± 0.01	0.83 ± 0.02	0.48 ± 0.11	0.95 ± 0.02	0.85 ± 0.02	0.94 ± 0.02	0.85 ± 0.01	0.7 ± 0.1	0.94 ± 0.03	0.45 ± 0.02	0.44 ± 0.01	0.45 ± 0.03	0.48 ± 0.02
[Al]	4.35 ± 0.04	4.37 ± 0.03	4.37 ± 0.03	4.61 ± 0.09	4.32 ± 0.03	4.39 ± 0.03	4.35 ± 0.04	4.36 ± 0.02	4.48 ± 0.05	4.36 ± 0.02	4.04 ± 0.04	4.02 ± 0.02	4.00 ± 0.03	4.06 ± 0.03
[Si]	32.2 ± 0.2	31.7 ± 0.1	32.1 ± 0.1	32.6 ± 0.1	31.8 ± 0.1	31.9 ± 0.1	31.7 ± 0.1	31.9 ± 0.1	32.1 ± 0.2	31.7 ± 0.1	33.8 ± 0.1	33.7 ± 0.1	34.01 ± 0.1	33.6 ± 0.1
[P]	0.042 ± 0.002	0.041 ± 0.001	0.048 ± 0.001	0.038 ± 0.001	0.04 ± 0.001	0.045 ± 0.002	0.042 ± 0.001	0.043 ± 0.001	0.043 ± 0.001	0.042 ± 0.001	0.026 ± 0.001	0.025 ± 0.002	0.026 ± 0.002	0.026 ± 0.001
[K]	1.03 ± 0.01	1.02 ± 0.01	1.15 ± 0.01	1.26 ± 0.06	1.08 ± 0.01	1.03 ± 0.01	1.02 ± 0.01	1.05 ± 0.01	1.03 ± 0.06	1.01 ± 0.03	1.47 ± 0.03	1.41 ± 0.03	1.53 ± 0.04	1.42 ± 0.03
[Ca]	2.05 ± 0.02	2.29 ± 0.02	1.77 ± 0.03	0.82 ± 0.33	2.20 ± 0.06	2.13 ± 0.03	2.36 ± 0.05	2.21 ± 0.03	1.78 ± 0.36	2.37 ± 0.02	1.32 ± 0.04	1.47 ± 0.04	1.21 ± 0.03	1.42 ± 0.02
[Ti]	0.31 ± 0.02	0.28 ± 0.01	0.32 ± 0.01	0.30 ± 0.01	0.29 ± 0.01	0.30 ± 0.01	0.28 ± 0.01	0.31 ± 0.01	0.27 ± 0.01	0.28 ± 0.01	0.18 ± 0.01	0.17 ± 0.01	0.18 ± 0.01	0.17 ± 0.01
[Mn]	0.053 ± 0.003	0.050 ± 0.002	0.061 ± 0.002	0.037 ± 0.005	0.047 ± 0.002	0.053 ± 0.002	0.047 ± 0.001	0.071 ± 0.001	0.045 ± 0.003	0.051 ± 0.0	0.034 ± 0.002	0.029 ± 0.001	0.034 ± 0.002	0.032 ± 0.002
[Fe]	1.08 ± 0.06	1.01 ± 0.01	1.19 ± 0.03	0.85 ± 0.09	1.00 ± 0.04	1.10 ± 0.03	1.02 ± 0.01	1.16 ± 0.01	1.02 ± 0.05	1.04 ± 0.03	0.65 ± 0.02	0.57 ± 0.01	0.64 ± 0.04	0.57 ± 0.01
Rb	65.2 ± 2.6	54.0 ± 1.1	78.8 ± 1.2	91.5 ± 9.0	60.2 ± 1.6	69.4 ± 1.3	55.8 ± 1.8	79.0 ± 0.1	72.6 ± 10.6	57.9 ± 0.9	91.3 ± 0.9	82.0 ± 1.1	98.2 ± 0.6	88 ± 2.1
Sr	435 ± 6.2	484.2 ± 8.5	362.1 ± 4.8	204.9 ± 66.2	480.3 ± 17.6	442.2 ± 5.2	523.1 ± 16.3	448.3 ± 3.0	411.9 ± 57.0	498.6 ± 3.2	302.8 ± 5.8	340.5 ± 6.8	291.7 ± 3.5	359.5 ± 9.6
Y	17.4 ± 0.9	12.7 ± 0.5	17.7 ± 0.4	15.4 ± 1.2	13.8 ± 0.3	16.1 ± 0.4	13.7 ± 0.9	16.5 ± 1	13.1 ± 1.1	15.4 ± 0.6	9.7 ± 0.3	10.1 ± 0.2	10.3 ± 0.7	10.4 ± 0.8
Zr	168 ± 12	134 ± 1	162 ± 4	153 ± 4	137 ± 4	144 ± 3	129 ± 2	138 ± 3	134 ± 3	128 ± 2	115 ± 2	115 ± 1	112 ± 5	114 ± 2
n[b]	9	6	6	3	4	14	5	3	3	3	8	6	9	4

[a] Average sample elevations reported next to site name in parentheses.
[b] n = number of samples.

~ 50 μm) and ignited in a muffle furnace at 550°C for 12 h, thus eliminating any organic material. Concentrations of Si, Al, Ca, Fe, Na, K, Ti, and other major rock-forming elements were measured from homogeneous glass disks that were fused from mixtures of 0.5 g powdered sample and 3.5 g $Li_2B_4O_7$ flux in platinum crucibles at ~ 1000°C [32]. Concentrations of Zr and other trace elements were measured from pressed, powdered samples (~ 3 g each, encased in boric acid binder). Element concentrations were measured by XRF using a Phillips model PW 2400.

The denudation rates used in our weathering rate estimates (in Eqs. 1 and 3) need to be spatially representative of our sampling areas, to ensure consistency with our CDF measurements, which are averaged over 0.5–1.0 ha scales. Several studies [18–20,31] have shown that cosmogenic nuclide concentrations in well-mixed sediment can be used to infer the average denudation rate of the sediment's source area, if denudation rates are fast enough that radioactive decay can be ignored. To apply this approach at our Santa Rosa Mountains climate transect, where half of our sampling sites were steep catchments and half were flatter, crestal areas, we sampled sediments from hollows (in two of the three catchment sites) and from widely distributed soil surfaces (in two of the three ridgecrest areas) for analysis of denudation rates by cosmogenic nuclide methods. Sediment from the hollows should be spatially representative of eroding material in the contributing area, as should manually mixed sediment from multiple soil surfaces on ridgetops.

To measure cosmogenic nuclide concentrations in quartz from our soils and sediments, we first isolated and purified the quartz in each sample using magnetic separation and selective mineral dissolution techniques [33,34], and then took subsamples of pure quartz (typically ~ 40 g) and added small amounts of ^{9}Be (typically ~ 0.5 mg). We then dissolved the subsampled quartz, extracted and purified its Be using ion exchange chromatography and selective precipitation, ignited the Be at 750°C to create BeO, and mixed the BeO with Nb. Be targets prepared from these mixtures were analyzed by accelerator mass spectrometry (AMS) on the tandem accelerator at

Lawrence Livermore National Laboratory (LLNL), thus yielding measurements of $^{10}Be/^{9}Be$ [35]. ^{10}Be concentrations were calculated by multiplying the $^{10}Be/^{9}Be$ ratios from AMS by the ^{9}Be concentrations determined from initial masses of quartz and added ^{9}Be.

4. Results and discussion

Average element concentrations for each of the sampling sites are reported in Table 1. Bedrock specimens and their element concentrations (Table 1) indicate that lithology is roughly uniform across the transect. However, the two highest sites along the transect, SR-3 and SR-10, have slightly higher concentrations of Si, K and Rb and slightly lower concentrations of Ca, Mg, Fe, Mn, Ti, Sr and Zr, indicating that there is some compositional zoning within the Santa Rosa granodiorite.

Characteristics such as altitude and average temperature along the transect are listed in Table 2, along with cosmogenic nuclide data, denudation rates, CDFs, chemical weathering rates and physical erosion rates. Our results show that CDFs decrease rapidly with increasing altitude (Fig. 2A), dropping from 0.20 at the base of the transect to near 0.0 at the top, above the upper limits of aspen and woody brush (indicated by the gray bands marked 'tree line' in Fig. 2).

By contrast, denudation rates, inferred from ^{10}Be concentrations at four of the six sites, span a range of only 104–144 t/km^2/yr (average = 117 t/km^2/yr) and show no clear trends with elevation (Fig. 2B). Hence, the supply rate of fresh minerals from denudation appears to be relatively uniform, compared to the CDFs, which show that soils are much less intensively weathered at higher altitudes. Hence, chemical weathering rates must be slower at higher altitudes, because significantly less-weathered soils are being produced under

Table 2
Study location characteristics and rates of denudation, chemical weathering and physical erosion[a]

ID	Average altitude (m)	Estimated mean air temperature[b] (°C)	Average hillslope gradient (m/m)	^{10}Be[c] (10^5 at/g)	Denudation rate[d] (t/km^2/yr)	CDF[e]	Chemical weathering rate (t/km^2/yr)	Physical erosion rate[f] (t/km^2/yr)
SR-10	2749	−0.4	0.55	N.A.[g]	117 ± 12[g]	−0.02 ± 0.05	−2 ± 6	119 ± 13
SR-3	2580	0.6	0.52	3.57 ± 0.20	132 ± 14	0.00 ± 0.02	0 ± 3	132 ± 14
SR-1	2377	1.8	ridgetop[h]	4.47 ± 0.25	106 ± 11	0.07 ± 0.02	7 ± 3	99 ± 11
SR-4	2350	2.0	0.48	3.26 ± 0.19	144 ± 15	0.10 ± 0.02	15 ± 5	129 ± 14
SR-6	2180	3.0	ridgetop[h]	4.54 ± 0.25	104 ± 11	0.16 ± 0.03	16 ± 5	87 ± 10
SR-7	2086	3.6	ridgetop[h]	N.A.[g]	117 ± 12[g]	0.20 ± 0.06	24 ± 7	93 ± 12

[a] Uncertainties are standard errors.
[b] Temperatures based on a lapse rate of −6°C/km and mean annual temperatures from nearby weather monitoring stations.
[c] ^{10}Be calculated from $^{10}Be/^{9}Be$ measured by AMS at LLNL, and standardized against ICN ^{10}Be prepared by K. Nishiizumi (personal communication).
[d] Details of our methods for estimating denudation rates from ^{10}Be concentrations (including nuclide production rates and scaling factors used here) are provided in the electronic appendix. To adjust cosmogenic nuclide production rates for attenuation by snow cover we assume that snow density = 0.4 g/cm^3, that snow cover increases linearly from 0 at SR-6 to 2 m at SR-3, and that it persists 4 months per year. Neglecting snow cover completely leads to denudation rates that are at most only ~15% higher than those listed here. Hence errors in our assumptions about density, depth, and average duration of snow cover would not lead to significant errors in denudation rates. Moreover, because CDFs decline rapidly with altitude, small errors in denudation rates near the top would have little effect on the pattern of chemical weathering rates shown in Fig. 2C.
[e] Calculated from $1-[Zr]_{rock}/[Zr]_{soil}$ using data from Table 1.
[f] Calculated from $D[Zr]_{rock}/[Zr]_{soil}$.
[g] No cosmogenic data are available for SR-7 or SR-10; denudation rates are assumed to be the average of the other four locations (see text).
[h] Ridgetop gradients are difficult to define precisely because surfaces are curved, but we estimate them to be 0.00 m/m, within uncertainties (± 0.03 m/m).

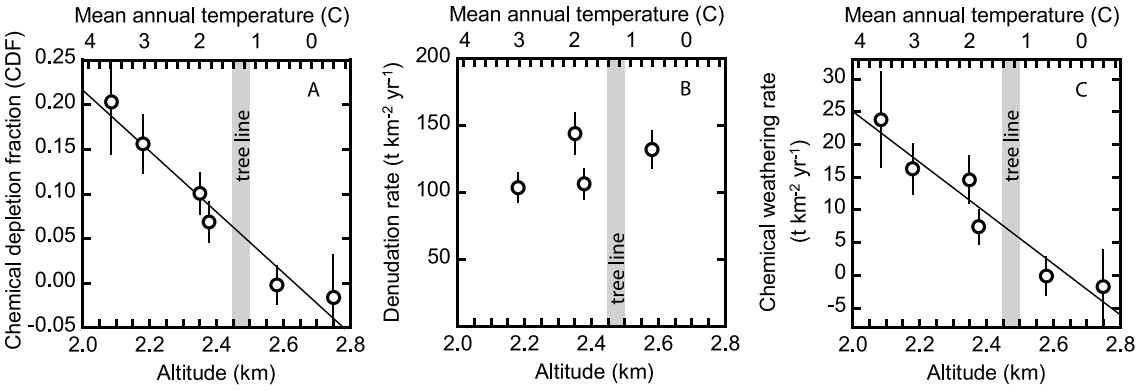

Fig. 2. CDFs, denudation rates and weathering rates plotted against altitude (lower axes) and temperature (upper axes). Vertical bar (labeled 'tree line') marks upper limits of aspen (*Populus tremuloides*) and woody brush (*Ceanothus*). Temperature–altitude relationship is based on a lapse rate of −6°C/km and mean annual temperatures from nearby weather monitoring stations. CDFs decrease from 0.2 to 0.0 (A), whereas denudation rates vary by a factor of <1.4 across the site (B), consistent with an increase in the dominance of physical erosion and decrease in chemical weathering rates (C) with increasing altitude. Lines through data in A and C are linear regressions. For calculating weathering rates at the highest and lowest sites (where no cosmogenic measurements are available), denudation rates were assumed to be the average of the other four sites. Note that because the CDF is 0 within error at the highest site, the weathering rate there must also be 0 within error, independent of the denudation rate (see text and Eq. 1).

roughly the same rates of supply of unweathered material. This is illustrated in Fig. 2C, which shows that chemical weathering rates drop off rapidly with increasing altitude, and are negligible above the upper limits of aspen and woody brush.

Note that, for calculating weathering rates at the highest and lowest sites (where no cosmogenic data are available), denudation rates were assumed to be the average of the other four sites. This should be reasonable; the consistency of denudation rates at the middle four sites and absence of obvious knickpoints in Hanson Creek together seem to imply that denudation rates along the transect are uniformly adjusted to a common baselevel lowering rate. Note also that because the CDF is 0 within error at the highest site, the weathering rate there must also be 0, independent of the denudation rate (see Eq. 1). Hence, the analyses and conclusions that follow would be unaffected in the unlikely case that denudation rates at the highest site were significantly higher or lower than what is assumed here.

Our cosmogenic nuclide and geochemical mass balance measurements are consistent with increasing dominance of physical erosion with increasing altitude, and indicate that chemical weathering is almost completely shut off in the sparsely vegetated areas at the top of the transect (Fig. 2). The negligible weathering rate at the highest sites is indicated by the lack of discernible Zr enrichment at SR-3 and SR-10 (Table 1), and is consistent with the observation that soils from the higher sites exhibit increasingly abundant proportions of fresh-looking mineral grains. The shutoff in chemical weathering above the vegetation transition also coincides with the transition to a more Si- and K-rich bedrock, as noted above from Table 1. Hence we cannot rule out the possibility that lithologic differences contribute to the patterns observed in Fig. 2A,C. However, the downward trends in CDFs and weathering rates would still be evident even if the highest sites were excluded from the analysis. Thus we can be reasonably certain that the sharp decline in weathering rates observed along the Santa Rosa Mountains transect arises largely from non-lithologic factors such as decreases in temperature, increases in the extent and depth (and thus duration) of snow cover, and changes in the density and type of vegetative cover.

Fig. 2A indicates that the fraction of denudation that is accounted for by chemical weathering decreases with increasing altitude and consequently that the fraction of denudation accounted

for by physical erosion increases over the same interval. This suggests that the effectiveness of physical erosion has increased as the effectiveness of chemical weathering has decreased. Field observations suggest that freeze–thaw-induced soil creep is an important sediment transport process along our transect, and it seems plausible that the observed increase in physical erosion rates (Table 2) could be at least partly accommodated by changes in freeze–thaw cycling, which one would expect to be more effective at higher (and thus wetter and colder) elevations. Due to increasingly sparse vegetative cover, other physical processes (such as rainsplash and shallow landsliding) could also be more effective at higher elevations. Hence, the increasing dominance of physical over chemical denudation with increasing altitude is generally consistent with what we might expect from field observations of erosional processes and climatic conditions along our transect.

Along our Santa Rosa Mountains transect, confounding variability in mineral supply from erosion of rock is minimal, because denudation rates vary by only a factor of 1.4 (Fig. 2B). This will not be the case everywhere. For example, previous work in the Sierra Nevada Mountains of California examined localities where denudation rates can vary by more than an order of magnitude within several kilometers, in response to local base-level forcing. In these localities, rates of chemical weathering and physical erosion are often tightly coupled, presumably because erosion controls the rate at which mineral surfaces are made available for chemical attack [13]. Results from our temperate Sierra Nevada sites [13] and tropical Rio Icacos [16] suggest that site-to-site differences in denudation rates can often obscure relationships between climate and chemical weathering rates [16]. However, our cosmogenic/mass balance approach is well suited for disentangling erosional effects from other factors, such as climate, because rates of chemical weathering and total denudation are measured together as part of the method. To the extent that supply rates of fresh minerals regulate chemical weathering rates, analysis of CDFs should provide a rational framework for quantifying climatic effects on chemical weathering rates of soils [13,16], as indicated by inspection of Eqs. 2 and 4. For example, CDF_X values calculated via Eq. 4 express elemental weathering rates that are normalized by the supply rate of element X to the soil (equal to the product of the overall denudation rate D and the concentration $[X]_{rock}$ of the element in the parent material). Hence, differences in a CDF_X across a series of sites should largely reflect factors such as climate, and not variations in rates of mineral supply, even if bedrock compositions and denudation rates vary substantially from place to place.

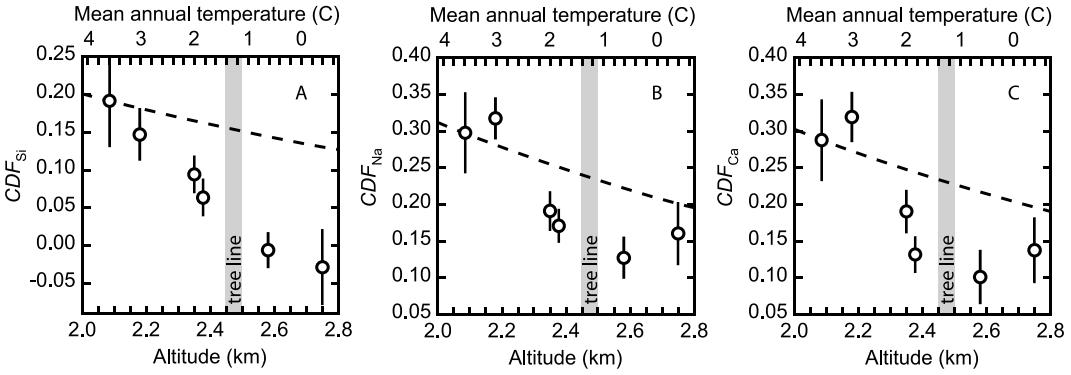

Fig. 3. CDFs of Si (A), Na (B) and Ca (C) plotted against altitude (lower axes) and temperature (upper axes). Dashed lines show altitudinal declines predicted by Arrhenius reaction kinetics (Eq. 6, with $\Delta E_X = 60$ kJ/mol). Weathering rates decline faster than one would predict from Eq. 6, based on the decrease in air temperature alone. The CDF of an individual element is its weathering rate normalized by its supply rate to the soil. Hence, trends in A, B and C should largely reflect effects of differences in non-supply-related factors, such as temperature, precipitation, and vegetation cover.

At the Santa Rosa Mountains transect, the CDFs of Si, Na, and Ca all decrease with increasing altitude and thus decreasing temperature (Fig. 3). Na and Ca at the highest locations are slightly depleted in soils, relative to rock, indicating that Na and Ca weather there (Fig. 3B,C), although the total mass loss is insufficient to significantly enrich zirconium concentrations in the soils (Fig. 2A).

How much of this decrease in chemical weathering rates can be attributed to the decrease in temperature as altitude increases? Silicate mineral weathering kinetics are conventionally modeled [10,36] using the Arrhenius equation:

$$W_X = A \exp\left[-\frac{\Delta E_X}{RT}\right] \quad (5)$$

where A is an empirical constant that subsumes the effects of surface area and surface reactivity, ΔE_X is the activation energy for the weathering reaction that releases element X, R is the universal gas constant, and T is absolute temperature in Kelvin. Although the Arrhenius equation is strictly applicable to the weathering kinetics of individual minerals, it has nevertheless been applied to elemental weathering rates as well [10,37], under the assumption that the weathering flux of an individual element will be dominated by dissolution of a single mineral, and thus will have a single activation energy. If we further assume that the pre-exponential factor A is proportional to the rate of mineral supply by denudation, we can estimate the effects of temperature on the CDFs at two different locations as:

$$\frac{CDF_{X,1}}{CDF_{X,2}} = \exp\left[\frac{\Delta E_X}{R}\left(\frac{1}{T_2}-\frac{1}{T_1}\right)\right] \quad (6)$$

where $CDF_{X,1}$ and $CDF_{X,2}$ are the CDFs of element X (from Eq. 4) at temperatures T_1 and T_2 (both in Kelvin), respectively. Typical activation energies for silicate mineral weathering in granitic rock are near 60 kJ/mol [10], implying that over the estimated 4 K temperature range for our Santa Rosa transect, CDFs should decline by roughly 32%, roughly two to three times less than what we observe (Fig. 3A–C). Hence, the normalized weathering rates plotted in Fig. 3 exhibit greater temperature dependence than one would predict from simple reaction kinetics using typical activation energies for silicate weathering.

The unexpectedly steep declines in CDFs (Fig. 3) suggest that weathering rates at Santa Rosa Mountains may also be affected by factors other than temperature, such as the progressive decline in vegetative cover and increase in snow cover and duration of freezing with altitude, which one might expect to be accompanied by significant changes in soil chemistry and soil microbiology. The fact that chemical weathering rates fall virtually to zero above the transition to sparse sagebrush (marked as 'tree line' in Figs. 2 and 3) is consistent with this hypothesis.

Our cosmogenic nuclide and geochemical mass balance techniques measure average rates of denudation and weathering over the millennial timescales of soil development, whereas instrumental records of climate measures span only years to decades. Climate averaged over the last several thousand years will differ from climate averaged over the last few years or decades. However, for several reasons, this discrepancy should have a relatively small effect on the results from our study. First, the differences in climate across the Santa Rosa Mountains transect are larger than plausible shifts in climate over the erosional timescales considered here; mean annual temperatures vary by up to 4°C across our climate transect, whereas, by comparison, in the White Mountains, nearby in the western USA, Late Holocene warming has only been about 2°C [38]. Second, while our climate data may not precisely reflect the long-term average climate, we can be certain the site-to-site differences in climate on which the analysis is based have been largely preserved, because the topography, lapse rates and other orographic effects that create them could not have not changed substantially. Third, climatic variations are unlikely to have had a large effect on the rate of fresh mineral supply to soils, given that hillslope denudation rates appear to be relatively insensitive to differences in climate, as indicated by cosmogenic nuclide data from a series of granitic catchments in the nearby Sierra Nevada Mountains, California [39]. Finally, changes in climate over the Holocene may have had a larger effect on soil development, but will be less impor-

Table 3
CDFs from Santa Rosa Mountains and six granitic sites in the Sierra Nevada[a]

Site name	Altitude (m)	Estimated mean air temperature (°C)	CDF
Santa Rosa Mountains (41.50°N; 2387 m; 65–85 cm/yr; 1.6°C; average CDF = 0.07 ± 0.04)[b]			
SR-10	2749	−0.4	−0.02 ± 0.05
SR-3	2580	0.6	0.00 ± 0.02
SR-1	2377	1.8	0.07 ± 0.02
SR-4	2350	2.0	0.10 ± 0.02
SR-6	2180	3.0	0.16 ± 0.03
SR-7	2086	3.6	0.20 ± 0.06
Sunday Peak, Sierra Nevada, USA (35.78°N; 2340 m; 105 cm/yr; 9.4°C; average CDF = 0.10 ± 0.04)			
SP-8	2423	8.9	0.12 ± 0.05
SP-3	2329	9.5	0.03 ± 0.08
SP-1	2273	9.8	0.11 ± 0.06
Adams Peak, Sierra Nevada, USA (39.83°N; 2106 m; 60 cm/yr; 4.2°C; average CDF = 0.14 ± 0.02)			
AP-11	2254	3.3	0.15 ± 0.06
AP-4	2193	3.7	0.06 ± 0.04
AP-3	2141	4.0	0.17 ± 0.02
AP-5	2048	4.5	0.12 ± 0.06
AP-13	1894	5.5	0.14 ± 0.04
Antelope Lake, Sierra Nevada, USA (41.17°N; 1760 m; 85 cm/yr; 7.8°C; average CDF = 0.18 ± 0.05)			
AL-9	1799	7.6	0.22 ± 0.11
AL-10	1799	7.6	0.14 ± 0.05
AL-4	1744	7.9	0.27 ± 0.07
AL-5	1691	8.2	0.22 ± 0.23
Fort Sage, Sierra Nevada, USA (41.17°N; 1490 m; 25 cm/yr; 12.2°C; average CDF = 0.15 ± 0.03)			
A1	1530	12.0	0.06 ± 0.05
A2(s)	1510	12.1	0.15 ± 0.04
A3(s)	1480	12.3	0.18 ± 0.05
A4(s)	1450	12.5	0.16 ± 0.03
Nichols Peak, Sierra Nevada, USA (35.55°N; 1150 m; 20 cm/yr; 15.4°C; average CDF = 0.25 ± 0.06)			
NP-18	1184	15.2	0.29 ± 0.08
NP-1	1122	15.6	0.22 ± 0.06
Fall River, Sierra Nevada, USA (39.67°N; 865 m; 145 cm/yr; 11.9°C; average CDF = 0.19 ± 0.02)			
FR-8	1056	10.7	0.18 ± 0.03
FR-2	927	11.5	0.15 ± 0.08
FR-6	869	11.9	0.19 ± 0.05
FR-5	597	13.5	0.21 ± 0.03

[a] Sierra Nevada data are from Riebe et al. ([13], their table 1).
[b] Site descriptions include average values for latitude, altitude, precipitation, temperature and CDF. Average CDF is weighted by inverse variance.

tant where soils are thinner and denudation rates are faster, because soil turnover times (measured by soil depth divided by denudation rate) will be shorter; for the average Santa Rosa Mountains denudation rate of 117 t/km^2/yr, a soil thickness of 60 cm (maximum) corresponds to a turnover time of only 6700 years (maximum), assuming a soil density of 1.3 g/cm^3, indicating that soils in the Santa Rosa Mountains never experienced full glacial conditions. Taken together these observations suggest that the sharp decline in chemical weathering rates observed along the Santa Rosa Mountains transect is not a relict of past climate, but instead can be readily associated with the site-to-site climatic contrasts that are observed today.

At Santa Rosa Mountains transect, several climatic factors apparently complement one another such that CDFs decline sharply over a short distance (Figs. 1–3). However, CDFs decline much less strongly with elevation across several lower, but climatically diverse, granitic sites in the Sierra Nevada Mountains (Table 3, after [13]). The Sier-

ra Nevada sites span 20–145 cm/yr in annual precipitation and 4–15°C in mean annual temperature, and consequently their vegetation densities and compositions vary widely as well. Yet Table 3 shows that, despite their diverse climates, their average CDFs range only between 0.10 and 0.25, whereas at the Santa Rosa Mountains transect, we observe a systematic decline from 0.20 to 0 along a much narrower climatic gradient. The sharp decline in CDFs observed along the Santa Rosa Mountains transect may be related to its high-altitude setting. Consistent with this conjecture is the observation that among the Sierra Nevada sites, the highest average altitude corresponds to the lowest average CDF (Sunday Peak, with average altitude = 2340 m and average CDF = 0.10 ± 0.04; see Table 3). Moreover, when CDFs are plotted against altitude for the entire data set (Fig. 4), a sharp altitudinal decline is only apparent above $\sim$2 km (including the two highest sites from the Sierra Nevada). The patterns shown in Fig. 4 suggest that chemical weathering rates may be particularly sensitive to differences in climate above a certain threshold altitude (in this case roughly 2 km), where changes in temperature, vegetation and snow cover apparently work together to enhance physical erosion while simultaneously retarding chemical weathering. The altitude of such a threshold would presumably vary from mountain range to mountain range, depending on latitude, local vegetation distributions, and topographic factors (including rain shadow effects, and orientation relative to prevailing storm patterns).

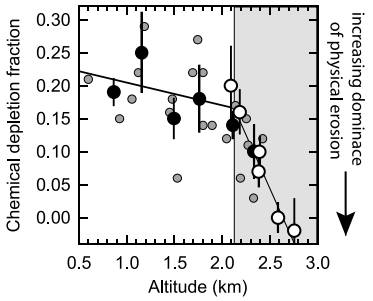

Fig. 4. CDF as a function of altitude for our Santa Rosa Mountains transect (open circles) and six locations in the Sierra Nevada (closed circles are location-wide averages and smaller, shaded circles are individual catchments; see Table 3). Lines are linear regression fits to average CDFs (data in clear and shaded regions were analyzed separately). Below 2.1 km (clear area), CDFs are not strongly correlated with altitude, despite wide variations in climate across the sites. Higher-elevation sites (shaded area) exhibit a steep decline in CDFs, consistent with increasing dominance of physical erosion. Chemical weathering rates appear to be particularly sensitive to altitudinal differences in climate above a threshold altitude of $\sim$2.1 km.

Documenting and quantifying the relative importance of the individual mechanisms that regulate chemical weathering rates across our transect is not the focus of this analysis (which aims to quantify the decrease in weathering rates itself). However, we can identify several plausible avenues for further research along these lines. For example, given that vegetation may contribute to mineral weathering in several ways – by retaining moisture, by altering soil acidity, by rooting into bedrock and thus helping to disaggregate it, or by supporting soil microbial communities that promote weathering of mineral surfaces – we suggest that measurements of soil moisture, acidity and microbial communities might be useful for explaining the unexpectedly sharp decline in weathering rates with altitude. Alternatively, if plants are sparse at the top of the transect because mineral weathering is slow, making rock-derived nutrients scarce, then measurements of soil solution chemistry and nutrient levels might provide more insight into the association between sparse vegetation and slow mineral weathering near the top of the transect. In any case, given the implications for chemical weathering rates of crystalline mountain ranges, the mechanisms underlying the sharp altitudinal decrease in chemical weathering rates measured here merit further study both in the Santa Rosa Mountains, and in other high-altitude settings where the phenomenon may also be important.

5. Conclusions and implications

Steep mountain ranges provide ideal settings for studying climatic effects on chemical weathering rates, because high relief and sharp differences in aspect will maximize site-to-site differences in climate, while minimizing the potentially con-

founding effects of differences in bedrock weathering susceptibility. Using cosmogenic nuclides in combination with a geochemical mass balance of soils and rock, as we did at the Santa Rosa Mountains transect, it is now possible to measure rates of physical erosion and chemical weathering together, and thus effectively account for site-to-site differences in the rates that minerals are supplied to soils by erosion of rock. Hence, our analysis of chemical weathering rates at the Santa Rosa Mountains transect at once effectively maximizes differences in the factor of interest (in this case, climate), while minimizing or accounting for potentially confounding variability in other factors (in this case, mineral supply rates).

Across our climate transect at the Santa Rosa Mountains transect, chemical weathering rates decline rapidly, from 24 to 0 t/km^2/yr, with increasing altitude, whereas denudation rates are much more uniform, varying by only a factor of 1.4. This is consistent with increasing dominance of physical erosion with increasing altitude, and indicates that chemical weathering is negligible at the top of the transect, above the upper limits of aspen and woody brush. As altitude increases, the CDFs of Si, Na and Ca decrease much more than one would expect from the decrease in average temperature alone, based on simple reaction kinetics. This implies that factors other than temperature – such as changes in vegetation type and density, and possibly also snow cover and depth – may play important roles in the sharp decline in chemical weathering rates at the Santa Rosa Mountains transect.

Previous measurements from six climatically diverse granitic sites in the Sierra Nevada Mountains indicate that average CDFs there span a range of only 0.10–0.25 [13], whereas at the Santa Rosa Mountains transect, we observe a systematic decline from 0.20 to 0.0 across a much narrower range of climatic conditions. The relationship between CDF and altitude for the combined set of Sierra Nevada and Santa Rosa data suggests that chemical weathering rates may be particularly sensitive to differences in elevation at higher sites, possibly due to climatic factors such as snow cover and vegetation. CDFs fall virtually to zero above the upper limits of trees and woody brush at the Santa Rosa Mountains transect, suggesting strong coupling between biological processes and chemical weathering rates in high-altitude crystalline terrain.

Acknowledgements

We thank L. Glaser and T. Teague for lab assistance and S. Binnie, W. Phillips and one anonymous reviewer for comments that helped us improve the manuscript. This work was supported by NSF Grant EAR-0000999 to J.W.K. ^{10}Be measurements were performed under the auspices of the U.S. Department of Energy by the University of California, Lawrence Livermore National Laboratory under contract W-7405-Eng-48. ***[KF]***

References

[1] R.A. Berner, A.C. Lasaga, R.M. Garrels, The carbonate-silicate geochemical cycle and its effect on atmospheric carbon-dioxide over the past 100 million years, Am. J. Sci. 283 (1983) 641–683.
[2] M.E. Raymo, W.F. Ruddiman, P.N. Froelich, Influence of late Cenozoic mountain building on ocean geochemical cycles, Geology 16 (1988) 649–653.
[3] T. Dunne, Rates of chemical denudation of silicate rocks in tropical catchments, Nature 274 (1978) 244–246.
[4] D.P. Dethier, Weathering rates and chemical fluxes from catchments in the Pacific Northwest USA, in: S.M. Coleman, D.P. Dethier (Eds.), Rates of Chemical Weathering of Rocks and Minerals, Academic, New York, 1986, pp. 503–528.
[5] J.I. Drever, J. Zobrist, Chemical weathering of silicate rocks as a function of elevation in the southern Swiss Alps, Geochim. Cosmochim. Acta 56 (1992) 3209–3216.
[6] J.I. Drever, The effect of land plants on weathering rates of silicate minerals, Geochim. Cosmochim. Acta 58 (1994) 2325–2332.
[7] K.L. Moulton, R.A. Berner, Quantification of the effect of plants on weathering: Studies in Iceland, Geology 26 (1998) 895–898.
[8] E.F. Kelly, O.A. Chadwick, T.E. Hilinski, The effect of plants on mineral weathering, Biogeochemistry 42 (1998) 21–53.
[9] N.E. Peters, Evaluation of environmental factors affecting yields of major dissolved ions of streams in the United States, U.S. Geol. Survey Water Supply Paper 2228, 1984.
[10] A.F. White, A.E. Blum, Effects of climate on chemical weathering in watersheds, Geochim. Cosmochim. Acta 59 (1995) 1729–1747.

[11] R.F. Stallard, J.M. Edmond, Geochemistry of the Amazon 2. The influence of geology and weathering environment on the dissolved load, J. Geophys. Res. 88 (1983) 9671–9688.
[12] J. Gaillardet, B. Dupre, P. Louvat, C.J. Allegre, Global silicate weathering and CO_2 consumption rates deduced from the chemistry of large rivers, Chem. Geol. 159 (1999) 3–30.
[13] C.S. Riebe, J.W. Kirchner, D.E. Granger, R.C. Finkel, Strong tectonic and weak climatic control of long-term chemical weathering rates, Geology 29 (2001) 511–514.
[14] S.P. Anderson, W.E. Dietrich, G.H. Brimhall, Weathering profiles, mass-balance analysis, and rates of solute loss; Linkages between weathering and erosion in a small steep catchment, Geol. Soc. Am. Bull. 114 (2002) 1143–1158.
[15] R. Millot, J. Gaillardet, B. Dupre, C.J. Allegre, The global control of silicate weathering rates and the coupling with physical erosion; new insights from rivers of the Canadian Shield, Earth Planet. Sci. Lett. 196 (2002) 83–98.
[16] C.S. Riebe, J.W. Kirchner, R.C. Finkel, Long-term rates of chemical weathering and physical erosion from cosmogenic nuclides and geochemical mass balance, Geochim. Cosmochim. Acta 67 (2003) 4411–4427.
[17] D. Lal, Cosmic ray labeling of erosion surfaces: in situ nuclide production rates and erosion models, Earth Planet. Sci. Lett. 104 (1991) 424–439.
[18] E.T. Brown, R.F. Stallard, M.C. Larsen, G.M. Raisbeck, F. Yiou, Denudation rates determined from the accumulation of in situ-produced ^{10}Be in the Luquillo Experimental Forest, Puerto Rico, Earth Planet. Sci. Lett. 129 (1995) 193–202.
[19] P. Bierman, E.J. Steig, Estimating rates of denudation using cosmogenic isotope abundances in sediment, Earth Surf. Proc. Landforms 21 (1996) 125–139.
[20] D.E. Granger, J.W. Kirchner, R.C. Finkel, Spatially averaged long-term erosion rates measured from in situ-produced cosmogenic nuclides in alluvial sediment, J. Geol. 104 (1996) 249–257.
[21] A.M. Heimsath, W.E. Dietrich, K. Nishiizumi, R.C. Finkel, The soil production function and landscape equilibrium, Nature 388 (1997) 358–361.
[22] C.S. Riebe, J.W. Kirchner, D.E. Granger, R.C. Finkel, Erosional equilibrium and disequilibrium in the Sierra Nevada, inferred from cosmogenic ^{26}Al and ^{10}Be in alluvial sediment, Geology 28 (2000) 803–806.
[23] J.W. Kirchner, D.E. Granger, C.S. Riebe, Cosmogenic isotope methods for measuring catchment erosion and weathering rates, J. Conf. Abstr. 2 (1997) 217.
[24] USDA-NRCS National Cartography and Geospatial Center, Nevada Annual Precipitation Map, 1988, scale 1:1,190,000.
[25] R. April, R. Newton, L.T. Coles, Chemical weathering in two Adirondack watersheds: Past and present day rates, Geol. Soc. Am. Bull. 97 (1986) 1232–1238.
[26] G.H. Brimhall, W.E. Dietrich, Constitutive mass balance relations between chemical composition, volume, density, porosity, and strain in metasomatic hydrochemical systems – Results on weathering and pedogenesis, Geochim. Cosmochim. Acta 51 (1987) 567–587.
[27] G.H. Brimhall, C.J. Lewis, C. Ford, J. Bratt, G. Taylor, O. Warin, Quantitative geochemical approach to pedogenesis importance of parent material reduction, volumetric expansion, and eolian influx in laterization, Geoderma 51 (1991) 51–91.
[28] G.H. Brimhall, O.A. Chadwick, C.J. Lewis, W. Compston, I.S. Williams, K.J. Danti, W.E. Dietrich, M.E. Power, D. Hendricks, J. Bratt, Deformational mass-transport and invasive processes in soil evolution, Science 255 (1992) 695–702.
[29] A.F. White, A.E. Blum, M.S. Schulz, D.V. Vivit, D.A. Stonestrom, M. Larsen, S.F. Murphy, D. Eberl, Chemical weathering in a tropical watershed, Luquillo mountains, Puerto Rico: I. Long-term versus short-term weathering fluxes, Geochim. Cosmochim. Acta 62 (1998) 209–226.
[30] E.E. Small, R.S. Anderson, G.S. Hancock, Estimates of the rate of regolith production using ^{10}Be and ^{26}Al from an alpine hillslope, Geomorphology 27 (1999) 131–150.
[31] D.E. Granger, C.S. Riebe, J.W. Kirchner, R.C. Finkel, Modulation of erosion on steep granitic slopes by boulder armoring, as revealed by cosmogenic ^{26}Al and ^{10}Be, Earth Planet. Sci. Lett. 186 (2001) 269–281.
[32] A.D. Karathanasis, B.F. Hajek, Elemental analysis by X-ray fluorescence spectroscopy, in: J.M. Bartels (Ed.) Methods of Soil Analysis, Part 3, Chemical Methods, SSSA Book Series 5, Soil Science Society of America and American Society of Agronomy, Madison, WI, 1996, pp. 161–223.
[33] C.P. Kohl, K. Nishiizumi, Chemical isolation of quartz for measurement of in situ-produced cosmogenic nuclides, Geochim. Cosmochim. Acta 56 (1992) 3583–3587.
[34] D.E. Granger, Landscape Erosion and River Downcutting Rates from Cosmogenic Nuclides in Sediment, Ph.D. Thesis, University of California, Berkeley, CA, 1996, 118 pp.
[35] J.C. Davis, I.D. Proctor, J.R. Southon, M.W. Caffee, D.W. Heikkinen, M.L. Roberts, T.L. Moore, K.W. Turteltaub, D.E. Nelson, D.H. Loyd, J.S. Vogel, LLNL/UC facility and research program, Nucl. Instr. Methods Phys. Res. B 52 (1990) 269–272.
[36] P.V. Brady, S.A. Carroll, Direct effects of CO_2 and temperature on silicate weathering: Possible implications for climate control, Geochim. Cosmochim. Acta 58 (1994) 1853–1856.
[37] A.F. White, A.E. Blum, T.D. Bullen, D.V. Vivit, M. Schulz, J. Fitzpatrick, The effect of temperature on experimental and natural chemical weathering rates of granitoid rocks, Geochim. Cosmochim. Acta 63 (1999) 3277–3291.
[38] V.C. LaMarche, Paleoclimatic inferences from long tree-ring records, Science 183 (1974) 1043–1048.
[39] C.S. Riebe, J.W. Kirchner, D.E. Granger, R.C. Finkel, Minimal climatic control on erosion rates in the Sierra Nevada, California, Geology 29 (2001) 447–450.